

A Simple and General Method for the Synthesis of Multicomponent $\text{Na}_2\text{V}_6\text{O}_{16}\cdot 3\text{H}_2\text{O}$ Single-Crystal Nanobelts

Jianguo Yu,^{†,‡} Jimmy C. Yu,^{*,†} Wingkei Ho,[†] Ling Wu,[†] and Xinchun Wang[†]

Department of Chemistry, The Chinese University of Hong Kong, Shatin, New Territories, Hong Kong, China, and State Key Laboratory of Advanced Technology for Materials Synthesis and Processing, Wuhan University of Technology, Wuhan, 430070, China

Received December 18, 2003; E-mail: jimyu@cuhk.edu.hk

Alkali-metal vanadium oxide bronzes with layered structures have attracted special attention due to their application as cathode materials in rechargeable high-energy-density lithium batteries and their diverse structural chemistry and properties.¹ $\text{Na}_2\text{V}_6\text{O}_{16}\cdot 3\text{H}_2\text{O}$ (barnesite) is a member of the Hewettite ($\text{M}_2\text{V}_6\text{O}_{16}\cdot n\text{H}_2\text{O}$, M = monovalent element or $\text{MV}_6\text{O}_{16}\cdot n\text{H}_2\text{O}$, M = divalent element) family.² $\text{Na}_2\text{V}_6\text{O}_{16}\cdot 3\text{H}_2\text{O}$ consists of V_3O_8 layers and interstitial hydrated Na ions. The V_3O_8 layer is composed of VO_6 octahedra and V_2O_8 units of edge-sharing square pyramids. The hydrated Na ions are located between the layers. Further structural details of the V_3O_8 layers have been described in the literature.³

Since the discovery of carbon nanotubes in 1991,⁴ one-dimensional (1D) nanostructured materials (nanotubes, nanobelts, nanowires, and nanorods) have attracted considerable attention due to their distinctive geometries, novel physical and chemical properties, and potential applications in numerous areas such as nanoscale electronics and photonics.⁵ Although many methods have been used to fabricate 1D objects, including electrochemistry,^{5b} templates (mesoporous silica, carbon nanotubes, etc.),^{5c} micro-emulsion-mediated systems,^{5d} arc discharge,⁴ laser-assisted catalysis growth,^{5e} solution,^{5f} vapor transport,^{5g} and solvothermal synthesis,^{5h} they suffer from the limits of high temperature, special equipment and conditions, or tedious procedures. Furthermore, these methods have mainly been concentrated on mono- and binary component structures, such as carbon,⁴ metals,^{6a} oxides^{6b} and II–VI,^{6c} III–V^{6d,6e} compounds, etc. However, only limited kinds of single-crystal ternary 1D nanostructures have been obtained until now, and the synthesis of new multicomponent 1D nanostructures remains challenging to materials scientists.^{2c,7} Recently, the belt-shaped 1D nanostructures have been intensively investigated due to the promising building-block function for nanoelectronics and optoelectronics,⁸ also, much effort has been devoted to developing new approaches to prepare these nanobelt materials.⁹ Here, we report for the first time that nanobelts of multicomponent $\text{Na}_2\text{V}_6\text{O}_{16}\cdot 3\text{H}_2\text{O}$ can be easily obtained by hydrothermal treatment of bulky V_2O_5 and NaF powders without using any templates or catalysts.

In a typical procedure, V_2O_5 (0.005 mol) and NaF (0.015 mol) powders were added into 70 mL of distilled water and stirred for 2 min. The slurry solution was placed in a 100-mL autoclave with a Teflon liner. The autoclave was maintained at 180 °C for 24 h and then air cooled to room temperature. After reaction, the pH value of the solution was 5.3. The brownish-red precipitate was collected and washed with distilled water and anhydrous alcohol several times. The final product was dried in a vacuum at 80 °C for 6 h.

An X-ray diffractometer (XRD, Bruker D8 Advance XRD with Cu K α radiation) was used to characterize the crystal structure of

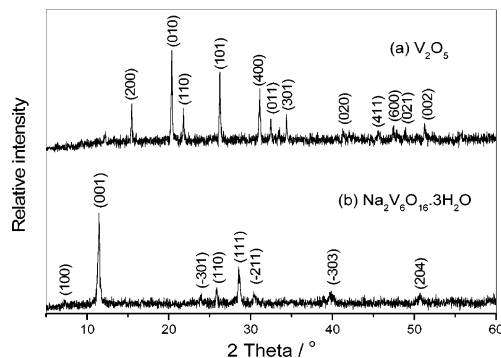


Figure 1. XRD patterns of (a) the starting material and (b) the product.

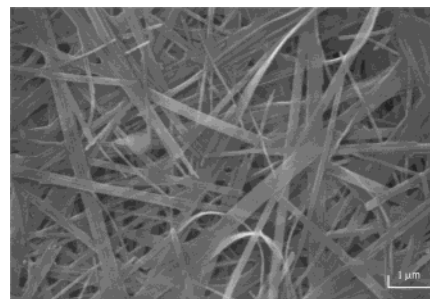


Figure 2. SEM images of the $\text{Na}_2\text{V}_6\text{O}_{16}\cdot 3\text{H}_2\text{O}$ nanobelts.

the products. Panels a and b of Figure 1 show the XRD patterns of the starting material and the nanobelt product, respectively. All the peaks in Figure 1b can be readily indexed to a pure monoclinic crystalline phase [space group: $P2_1/m$] of $\text{Na}_2\text{V}_6\text{O}_{16}\cdot 3\text{H}_2\text{O}$ with calculated lattice contents $a = 12.01(3)$ Å, $b = 3.71(2)$ Å, $c = 7.70(4)$ Å, $\beta = 94.90(3)^\circ$, which are in good agreement with the literature values (JCPDS No. 16-601). X-ray photoelectron spectroscopy (XPS) spectra (see Supporting Information) show that the nanobelts consist of Na, V, and O in a ratio of 1:2.99:9.61. Furthermore, a $\text{V}2p_{3/2}$ binding energy of 517.2 eV is characteristic of V^{+5} . Thermogravimetric analysis (TGA) measurements (see Supporting Information) reveal a 7.8% weight loss from 100 to 360 °C. This matches the water content of $\text{Na}_2\text{V}_6\text{O}_{16}\cdot 3\text{H}_2\text{O}$ (8.16%). The results from XRD, XPS, and TGA studies leave no doubt that the product is $\text{Na}_2\text{V}_6\text{O}_{16}\cdot 3\text{H}_2\text{O}$.

The morphology and size of the resulting product are shown in the scanning electron microscope (SEM, LEO 1450VP with an energy-dispersive X-ray fluorescence analyzer) images (Figure 2). Through the hydrothermal treatment, V_2O_5 powders of several micrometers in size react with NaF to produce belt-like materials of width around 60 to 500 nm and length of tens of microns. The rectangle-like cross section of the materials is clearly visible in the SEM image. The thickness of the belts ranges from more than 10

[†] The Chinese University of Hong Kong.

[‡] Wuhan University of Technology.

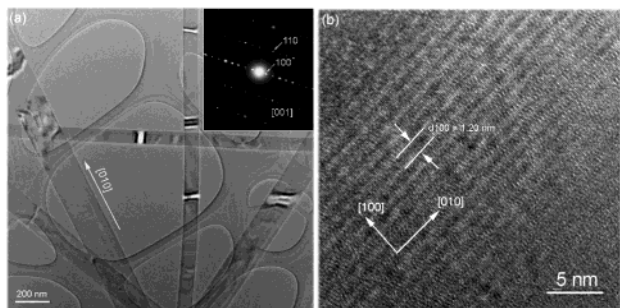
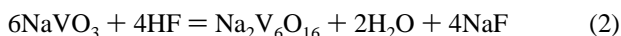
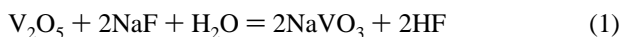


Figure 3. (a) TEM images of the resulting products and SAED pattern (inset of a) taken from a single nanobelt. (b) HRTEM image of an individual nanobelt.

to tens of nanometers, as estimated from the SEM images, and the width-to-thickness ratios are about 5 to 15. The yield and phase purity of the nanobelts are estimated to be higher than 90 and 95%, respectively, based on the SEM and XRD results. Energy-dispersive X-ray (EDX) analysis also shows that there is no fluorine in the resulting product.

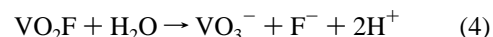
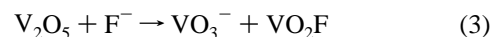
The belt-like structures of the products were further examined using transmission electron microscopy (TEM) and high-resolution transmission electron microscopy (HRTEM) (JEOL-2010F at 200 kV). Figure 3a shows the low magnification TEM image of typical $\text{Na}_2\text{V}_6\text{O}_{16}\cdot 3\text{H}_2\text{O}$ nanobelts. As can be seen from Figure 3a, the nanobelts show uniform width over their entire lengths, and some of the nanobelts stick together. The selected area electron diffraction (SAED) pattern (inset in Figure 3a) taken from a single nanobelt and recorded from the [001] zone axis indicates that the nanobelts are single crystals with a preferential growth direction along the [010] direction. Figure 3b is a representative HRTEM image of a single-crystalline $\text{Na}_2\text{V}_6\text{O}_{16}\cdot 3\text{H}_2\text{O}$ nanobelt, which shows the clearly resolved interplanar distance $d_{100} = 1.20$ nm and further confirms that the nanobelts grow along the [010] direction.

Additional studies have shown that it is possible to prepare other 1D nanomaterials including ammonium, alkali-metal, or alkali-earth metal vanadium oxide bronze hydrated compounds (such as $(\text{NH}_4)_2\text{V}_6\text{O}_{16}\cdot n\text{H}_2\text{O}$, $\text{K}_2\text{V}_6\text{O}_{16}\cdot n\text{H}_2\text{O}$, $\text{MgV}_6\text{O}_{16}\cdot n\text{H}_2\text{O}$, etc.) and transition metal oxyfluorides (e.g., $\text{ZnF}(\text{OH})$). We believe that this facile hydrothermal route, which uses bulky oxide and fluoride powders as precursors, is a general method for the synthesis of various multicomponent 1D nanomaterials. Although the exact formation mechanism for these 1D nanobelts is still unclear, it is obvious that the growth of the nanobelts is not template-directed. Since the raw materials used in our synthesis are oxides and fluorides, it is possible that $\text{Na}_2\text{V}_6\text{O}_{16}\cdot 3\text{H}_2\text{O}$ single-crystalline nanobelts are formed by a reaction-crystallization process (RC), in which bulky V_2O_5 particles react with NaF to form water-soluble NaVO_3 in solution under hydrothermal treatment. NaVO_3 is then polymerized to form $\text{V}_6\text{O}_{16}^{2-}$ ions. The unreacted V_2O_5 particles serve as the sites for the heterogeneous nucleation of the nanobelts, which subsequently crystallize along the [010] direction of $\text{Na}_2\text{V}_6\text{O}_{16}\cdot 3\text{H}_2\text{O}$ single crystals and grow into belt-shaped structures through a reaction-crystallization mechanism. The whole reaction process can be expressed as follows:



It is obvious that the reaction products rather than the raw materials are the precursors for further crystal growth. This is an important difference to the previous methods based on a vapor-

solid (VS)^{6b} or solution-solid (SS)¹⁰ process for nanobelt growth. Controlled experiments were carried out to investigate the influence of F^- ions on the synthesis of $\text{Na}_2\text{V}_6\text{O}_{16}\cdot 3\text{H}_2\text{O}$ nanobelts. It was found that the presence of F^- ions is crucial for the formation of $\text{Na}_2\text{V}_6\text{O}_{16}\cdot 3\text{H}_2\text{O}$ nanobelts. Without F^- ions or in the presence of other anions such as Cl^- , Br^- , NO_3^- , and SO_4^{2-} , the 1D nanobelts could not be obtained. This can be ascribed to the fact that F^- ions can enhance the dissolution and reaction of V_2O_5 by nucleophilic substitution.¹¹



In conclusion, we have developed a general hydrothermal reaction-crystallization route using bulky powders as precursors to synthesize uniform multicomponent $\text{Na}_2\text{V}_6\text{O}_{16}\cdot 3\text{H}_2\text{O}$ single-crystalline nanobelts on a large scale. This new strategy could be extended to prepare other multicomponent 1D nanomaterials including ammonium, alkali-metal or alkali-earth metal vanadium oxide bronze hydrated compounds and other transition metal oxyfluoride products. This is an efficient and mild solution method with clear advantages over the traditional high-temperature approach for the large-scale production of 1D multicomponent nanomaterials.

Acknowledgment. This work was supported by the NSFC (No. 50272049) and ITF (ITS/118/01).

Supporting Information Available: Detailed XPS and TGA characterization results (PDF). This material is available free of charge via the Internet at <http://pubs.acs.org>.

References

- (1) (a) Jouanneau, S.; Verbaere, A.; Guyomard, D. *J. Solid State Chem.* **2003**, *172*, 116. (b) Kumagai, N.; Yu, A.; West, K. *J. Appl. Electrochem.* **1997**, *27*, 953.
- (2) (a) Malcolm, R. *Am. Mineral.* **1955**, *40*, 322. (b) Weeks, A. D.; Ross, D. R.; Marvin, R. F. *Am. Mineral.* **1963**, *48*, 1187. (c) Kong, L.; Shao, M.; Xie, Q.; Liu, J.; Qian, Y. *J. Cryst. Growth* **2004**, *260*, 435.
- (3) (a) Wadsley, A. D. *Acta Crystallogr.* **1957**, *10*, 261. (b) Zavalij, P. Y.; Whittingham, M. S. *Acta Crystallogr. B* **1999**, *55*, 627.
- (4) Iijima, S. *Nature* **1991**, *354*, 56.
- (5) (a) Alivisatos, A. P. *Science* **1996**, *271*, 933. (b) Zhou, Y.; Yu, S. H.; Cui, X. P.; Wang, C. Y.; Chen, Z. Y. *Chem. Mater.* **1999**, *11*, 545. (c) Martin, C. R. *Science* **1994**, *226*, 1961. (d) Cao, M. H.; Hu, C. W.; Wang, E. B. *J. Am. Chem. Soc.* **2003**, *125*, 11196. (e) Morales, A. M.; Lieber, C. M. *Science* **1998**, *279*, 208. (f) Trentler, T. J.; Hickman, K. M.; Goel, S. C.; Viano, A. M.; Gibbons, P. C.; Buhro, W. E. *Science* **1995**, *270*, 1791. (g) Wu, Y.; Yang, P. *Chem. Mater.* **2000**, *12*, 605. (h) Doble, A.; Ngala, K.; Yang, S.; Zavalij, P. Y.; Whittingham, M. S. *Chem. Mater.* **2001**, *13*, 4382.
- (6) (a) Li, Y. D.; Wang, J.; Deng, Z.; Wu, Y.; Sun, X.; Yu, D.; Yang, P. *J. Am. Chem. Soc.* **2001**, *123*, 9904. (b) Pan, Z. W.; Dai, Z. R.; Wang, Z. L. *Science* **2001**, *291*, 1947. (c) Deng, Z. X.; Li, L. B.; Li, Y. D. *Inorg. Chem.* **2003**, *42*, 2331. (d) Duan, X. F.; Lieber, C. M.; *J. Am. Chem. Soc.* **2000**, *122*, 188. (e) Goldberger, J.; He, R. R.; Zhang, Y. F.; Lee, S. W.; Yan, H. Q.; Choi, H. J.; Yang, P. *Nature* **2003**, *422*, 599.
- (7) (a) Wang, J.; Li, Y. D. *Chem. Commun.* **2003**, 2320. (b) Yu, S. H.; Liu, B.; Mo, M. S.; Huang, J. H.; Liu, X. M.; Qian, Y. T. *Adv. Funct. Mater.* **2003**, *13*, 639. (c) Urban, J. J.; Yun, W. S.; Gu, Q.; Park, H. J. *Am. Chem. Soc.* **2002**, *124*, 1186. (d) Kang, Z. H.; Wang, E. B.; Jiang, M.; Lian, S. Y.; Li, Y. G.; Hu, C. W. *Eur. J. Inorg. Chem.* **2003**, 370. (e) Zhang, L.; Yu, J. C.; Xu, A. W.; Li, Q.; Kwong, K. W.; Wu, L. *Chem. Commun.* **2003**, 2910.
- (8) (a) Comini, E.; Faglia, G.; Sberveglieri, G.; Pan, Z. W.; Wang, Z. L. *Appl. Phys. Lett.* **2002**, *81*, 1869. (b) Li, Y. B.; Bando, Y.; Golberg, D.; Kurashima, K. *Appl. Phys. Lett.* **2002**, *81*, 5048.
- (9) (a) Hu, J. Q.; Ma, X. L.; Shang, N. G.; Xie, Z. Y.; Wang, N. B.; Lee, C. S.; Lee, S. T. *J. Phys. Chem. B* **2002**, *106*, 3823. (b) Li, X. L.; Liu, J. F.; Li, Y. D. *Appl. Phys. Lett.* **2002**, *81*, 4832. (c) Sun, X. M.; Chen, X.; Li, Y. D. *Inorg. Chem.* **2002**, *41*, 4996. (d) Wang, Z. L.; Pan, Z. W. *Adv. Mater.* **2002**, *14*, 1029.
- (10) Xu, A. W.; Fang, Y. P.; You, L. P.; Liu, H. Q. *J. Am. Chem. Soc.* **2003**, *125*, 1494.
- (11) (a) Sun, X. M.; Li, Y. D. *Chem. Commun.* **2003**, 1768. (b) Yu, J. C.; Yu, J.; Ho, W.; Jiang, Z.; Zhang, L. *Chem. Mater.* **2002**, *14*, 3808.

JA031795N